# Wortmannin Alters the Transferrin Receptor Endocytic Pathway In Vivo and In Vitro

David J. Spiro,* Werner Boll,† Tomas Kirchhausen,*† and
Marianne Wessling-Resnick*‡

*Program in Biological and Biomedical Sciences, Harvard Medical School, Boston, Massachusetts
02115; and †Department of Cell Biology, Harvard Medical School and The Center for Blood Research,
Boston, Massachusetts 02115

Treatment with the phosphatidylinositol 3-kinase inhibitor wortmannin promotes ~30% decrease in the steady-state number of cell-surface transferrin receptors. This effect is rapid and dose dependent, with maximal down-regulation elicited within 30 min of treatment and with an $IC_{50}$ ~25 nM wortmannin. Wortmannin-treated cells display an increased endocytic rate constant for transferrin internalization and decreased exocytic rate constants for transferrin recycling. In addition to these effects in vivo, wortmannin is a potent inhibitor ($IC_{50}$ ~15 nM) of a cell-free assay that detects the delivery of endocytosed probes into a common compartment. Inhibition of the in vitro assay involves the inactivation of a membrane-associated factor that can be recruited onto the surface of vesicles from the cytosol. Its effects on the cell-free assay suggest that wortmannin inhibits receptor sorting and/or vesicle budding required for delivery of endocytosed material to "mixing" endosomes. This idea is consistent with morphological changes induced by wortmannin, which include the formation of enlarged transferrin-containing structures and the disruption of the perinuclear endosomal compartment. However, the differential effects of wortmannin, specifically increased transferrin receptor internalization and inhibition of receptor recycling, implicate a role for phosphatidylinositol 3-kinase activity in multiple sorting events in the transferrin receptor's membrane traffic pathway.

## INTRODUCTION

The discovery that the yeast *VPS34* gene is necessary for sorting and traffic of vacuolar proteins has promoted interest in the role of lipid kinases in membrane traffic (Herman and Emr, 1990; Schu *et al.*, 1993). Vps34p has both phosphatidylinositol (PI)[1]-specific phosphatidylinositol 3-kinase (PI 3-kinase) and serine/threonine protein kinase activities (Stack and Emr, 1994) and shares significant homology with the p110 subunit of the mammalian PI 3-kinase (Hiles *et al.*, 1992). Complementation analysis has revealed that *end12*, a yeast mutant with defects in endocytic sorting mechanisms, has an altered *VPS34* gene (Munn and Riezman, 1994). Since the onset of the vacuolar sorting defect in temperature-sensitive *vps34* mutants correlates with a decrease in phosphatidylinositol 3-phosphate levels (Stack *et al.*, 1995), a requirement for phosphatidylinositol 3-phosphate in both endocytic and

---

‡ Corresponding author: Department of Nutrition, Harvard School of Public Health, 665 Huntington Ave, Boston, MA 02115.

[1] Abbreviations used: AP, clathrin assembly protein; Av$\beta$Gal, avidin-conjugated $\beta$-galactosidase; BSA, bovine serum albumin; B-Tf, biotinylated transferrin; DMSO, dimethylsulfoxide; FITC, fluorescein isothiocyanate; HEPES, (*n*-[2-hydroxyethyl] piperazine-*N'*-[2-ethanesulfonic acid]; IgG, immunoglobulin; IN/SUR, the ratio between internalized ligand and cell-surface bound ligand; $k_e$, endocytic rate constant; LAMP-1, lysosome associated protein 1; M6PR, cation-independent mannose 6-phosphate receptor; PBS, phosphate-buffered saline; PI, phosphatidylinositol; PI 3-kinase, phosphatidylinositol 3-kinase; PNS, post-nuclear supernatant; PDGF, platelet-derived growth factor; TBS, Tris-buffered saline; Tf, transferrin; TfR, transferrin receptor; TGN, trans-Golgi network.

vacuolar membrane traffic events in *Saccharomyces cerevisiae* is suggested. A role for PI 3-kinase activity has also been identified in the endocytic pathway of mammalian cells in studies of platelet-derived growth factor (PDGF) receptor traffic. Although wild-type PDGF receptors are delivered to a juxtanuclear compartment where they are ultimately degraded, mutant PDGF receptors lacking high-affinity binding sites for the SH2 domain of the p85/110 PI 3-kinase complex fail to reach lysosomes and instead become distributed to the cell's periphery (Joly *et al.*, 1994). Moreover, although lysosomal degradation of the mutant receptors is markedly decreased, internalization of these receptors is only slightly reduced. Thus, the activity of the p85/110 PI 3-kinase has been proposed to function in PDGF receptor endocytosis, presumably after initial clathrin-coated vesicle formation and budding, to regulate an activity involved in the fusion, sorting, and traffic of vesicles containing endocytosed material (Joly *et al.*, 1994). In contrast, the recent cloning of a mammalian homologue of Vps34p has led to speculation that this PI-specific PI 3-kinase may play a role in regulation of endosomal and lysosomal traffic in higher eukaryotes (Volinia *et al.*, 1995). This prediction is bolstered by the finding that the mammalian Vps34p is found in a complex with a homologue of Vps15p (Volinia *et al.*, 1995), a serine/threonine protein kinase that has been demonstrated to act upstream of Vps34p in the regulation of vacuolar protein sorting in yeast (Stack *et al.*, 1993, 1995).

The fungal metabolite wortmannin has been useful in further characterizing the role of PI 3-kinases in vesicle traffic. Wortmannin is an irreversible inhibitor that acts in the nanomolar range to block the activity of the p85/p110 PI 3-kinase of mammalian cells (Arcaro and Wymann, 1993; Powis *et al.*, 1994), as well as the mammalian Vps34p homologue (Volinia *et al.*, 1995). This inhibitor blocks insulin-stimulated translocation and fusion of vesicles containing glucose transporters with the plasma membrane (Clark *et al.*, 1994; Okada *et al.*, 1994) and the insulin-dependent exocytosis of IGF-2 and transferrin receptors (TfRs) (Sheperd *et al.*, 1995). Sorting of newly synthesized lysosomal enzymes from the trans-Golgi network to lysosomes (Brown *et al.*, 1995; Davidson, 1995) and transcytosis in polarized epithelial cells (Hansen *et al.*, 1996) are also disrupted by wortmannin. Several recent studies have shown that wortmannin directly affects the endocytic pathway as well; Joly *et al.* (1995) demonstrated that wortmannin abolishes ligand-induced degradation of the PDGF receptor, while Clague *et al.* (1995) characterized the inhibition of fluid phase endocytosis by the drug. Furthermore, Brown *et al.* (1995) have shown that wortmannin causes a down-regulation of surface mannose 6-phosphate receptors (M6PRs) but does not interfere with receptor internalization.

These studies implicating a PI 3-kinase activity in the regulation of both ligand-induced and fluid-phase endocytosis prompted us to examine the effects of wortmannin on membrane traffic of the constitutively recycling TfR. TfRs deliver iron to cells through a continual cycle that shuttles the ligand Tf between the plasma membrane and endosomal compartments. Internalization of the ligand-receptor complex is initiated via clathrin-coated vesicles, followed by delivery of Tf to the tubulovesicular endosomal network (Geuze *et al.*, 1984). After dissociation of iron in these acidic compartments, the apoTf-TfR complex is segregated from lysosomally directed molecules to be directed back to the cell surface (Dautry-Varsat *et al.*, 1983; Klausner *et al.*, 1983a). Recycling receptors such as the TfR and lysosomally targeted ligands and receptors are internalized by the same clathrin-mediated pathway and intermix in common early endosomal compartments (Geuze *et al.*, 1984; Salzman and Maxfield *et al.*, 1988). However, the pathways of these molecules diverge at sorting endosomes (Yamashiro *et al.*, 1984; Yamashiro and Maxfield, 1987); while lysosomally directed molecules are targeted to late endosomes, recycling receptors are sorted to the cell surface from a distinct class of recycling endosomes (Yamashiro *et al.*, 1984).

Our investigation demonstrates that the PI 3-kinase inhibitor wortmannin interferes with the TfR's membrane traffic pathway at multiple steps. Treatment of K562 cells with the drug induces a 30% decrease in cell-surface TfRs. Receptor down-regulation is associated with increased endocytosis and decreased exocytosis. In addition, wortmannin inhibits a cell-free assay reconstituting intracellular membrane sorting and fusion events. The fungal metabolite also alters the morphology of Tf-containing endosomes in HeLa cells. Thus, a role for PI 3-kinase activity is implicated in several discrete events of TfR traffic, including its recognition and delivery to the cell's interior, and sorting and recycling to the cell surface.

## MATERIALS AND METHODS

### Materials

Pfeffer (Stanford University School of Medicine, Stanford, CA). Human Texas Red-Tf was purchased from Molecular Probes (Eugene, OR), and fluorescein isothiocyanate (FITC)-conjugated goat anti-mouse immunoglobulin (IgG) antibody was obtained from Boehringer-Mannheim.

## $^{125}I$-Tf Binding Assay

Ligand binding studies were performed as previously described (Schonhorn and Wessling-Resnick, 1994). Briefly, K562 cells were treated with or without 100 nM wortmannin at 37°C in α-MEM containing 7.5% fetal bovine serum for the times indicated in the figure legends. Cells were subsequently chilled on ice, washed three times with ice-cold phosphate-buffered saline (PBS), and then resuspended in ice-cold binding buffer (25 mM (n-[2-hydroxyethyl] piperazine-N'-[2-ethanesulfonic acid] [HEPES], pH 7.4, 150 mM NaCl, 1 mg/ml bovine serum albumin [BSA]) at $10^7$ cells/ml. Binding reactions were prepared with 200 μl aliquots of this cell suspension, 25 μl binding buffer containing 5–500 nM $^{125}I$-Tf, and 25 μl binding buffer with or without 50 μM unlabeled Tf. Samples were incubated at 4°C for 60 min and then pelleted at 14,000 × g for 5 min. Following a brief wash with ice-cold PBS, cell-associated radioactivity was measured using a Beckman 8000 γ-counter (Beckman Instruments, Fullerton, CA); the amount of nonspecifically bound $^{125}I$-Tf associated in the presence of excess unlabeled Tf was subtracted from samples incubated in the absence of cold ligand to determine the amount of specific $^{125}I$-Tf bound (B). To determine the amount of free radiolabeled ligand (F), supernatants from the latter samples were also counted. Scatchard analysis was employed to determine the number of Tf binding sites (Scatchard, 1949).

The total number of cellular TfRs were determined as described by Klausner et al. (1983b). Briefly, K562 cells were solubilized in Tris-buffered saline TBS (10 mM Tris, pH 7.4, 150 mM NaCl) containing 0.1% Triton X-100. Fifty microliters of TBS with $^{125}I$-Tf (0.5–500 nM) and 50 μl of TBS with or without 50 μM unlabeled Tf were added to 150 μl aliquots of this cell extract. After a 10-min incubation at room temperature, 250 μl ice-cold 60% (w/v) ammonium sulfate was added to the binding reactions to precipitate the ligand-receptor complexes. After 5 min on ice, the precipitate was collected by filtration through Whatman GF/C filters and washed three times with 30% ammonium sulfate containing 0.8% BSA. Filters were dried, counted, and specific radioactivity was taken as the difference between radioactivity measured for samples incubated in the absence and presence of unlabeled Tf.

## IN/SUR Analysis of Endocytosis

Wortmannin-treated and control K562 cells were washed and resuspended at a concentration of 2 × $10^7$ cells/ml in ice-cold uptake buffer (25 mM HEPES, pH 7.4, 150 mM NaCl, 1 mg/ml BSA, 1 mg/ml glucose). Endocytosis of $^{125}I$-Tf was initiated by rapidly mixing 50 μl aliquots containing $10^6$ cells with 200 μl prewarmed uptake buffer containing 25 nM Tf. Uptake was terminated at the appropriate times (1–20 min) by placing the samples on ice followed by immediate centrifugation. Duplicate samples were quenched in parallel to measure total and internal $^{125}I$-Tf for each timepoint. To determine total cell-associated radioactivity, supernatants were aspirated and the cpm contained in the cell pellets was measured. The amount of internalized ligand (IN) was determined for the duplicate sample of cells, which were also pelleted but then resuspended in 100 μl 25 mM HEPES, pH 7.4, 150 mM NaCl. These cells were subsequently washed with 1 ml ice-cold 200 mM acetic acid, 150 mM NaCl (pH 2.7) for 2 min at 4°C to remove surface-bound radiolabel. Samples were immediately centrifuged and washed with PBS; supernatants were removed and pellets were counted to determine cell-associated radioactivity. Surface-bound ligand (SUR) was calculated as the difference between total and intracellular cpm measured in parallel samples. The ratio of internalized to surface ligand (IN/SUR) yields a biphasic curve when plotted as a function

of time (Wiley and Cunningham, 1982). The slope of the initial linear portion of the curve (0–5 min) was calculated by linear regression to determine the endocytic rate constant $k_e$.

## Kinetic Analysis of Exocytosis

K562 cells were incubated in the presence of 25 nM $^{125}I$-Tf with or without 100 nM wortmannin for 1 h. Cells were pelleted, washed once with ice-cold PBS, and surface-bound $^{125}I$-Tf was removed by a brief wash in 2 ml ice-cold 0.2 M acetate, pH 4.6, 150 mM NaCl for 2 min. The acid wash was immediately quenched by addition of 48 ml PBS; cells were washed three times with ice-cold PBS, and then resuspended in uptake buffer containing 250 nM unlabeled Tf with or without 100 nM wortmannin. Samples containing $10^6$ cells were incubated at 37°C for 1–60 min to permit Tf recycling, then immediately transferred to ice and washed once in ice-cold PBS. Cell-associated radioactivity was measured as described above.

Semilog plots of the percent cell-associated radioactivity remaining as a function of time were biphasic, indicating that exocytic release occurs from at least two compartments in K562 cells (Snider and Rogers, 1985; Stein and Sussman, 1986; Schonhorn and Wessling-Resnick, 1994). Assuming recycling from two separate exocytic compartments, the apparent first order rate constants for each were obtained by nonlinear curve fitting (Sigma Plot, Jandel Scientific) to the following equation: $y = a_f e^{k_f t} + a_s e^{k_s t}$, wherein $a_f$ and $a_s$ are the relative amounts of intracellular ligand within each compartment before exocytosis, and $k_f$ and $k_s$ represent apparent first-order rate constants for each compartment.

## Assay Conditions for Monitoring Colocalization of Endocytic Probes In Vitro

Cell-free assays were performed as previously described (Wessling-Resnick and Braell, 1990). Post-nuclear supernatants (PNS) were prepared from ~4 × $10^8$ K562 cells incubated for 60 min at 20°C in 2 ml uptake buffer (25 mM HEPES, pH 7.4, 150 mM NaCl, 1 mg/ml glucose, 1 mg/ml BSA) containing either 0.5 mg/ml AvβGal or 100 nM B-Tf. Internalization was quenched by addition of 10 ml ice-cold PBS, and cells were extensively washed in PBS. The cells were then resuspended in three volumes of ice-cold breaking buffer (20 mM HEPES, pH 7.4, 0.1 M KCl, 85 mM sucrose, 20 μM EGTA) and broken using a stainless steel ball homogenizer. PNS was collected by centrifugation at 800 × g for 5 min at 4°C. To separate vesicle fractions, PNS was layered over 0.25 M sucrose, 10 mM acetic acid, 10 mM triethanolamine, 1 mM EDTA, adjusted to pH 7.4, and membranes were pelleted onto a cushion of isotonic Nycodenz (Accurate Chemicals, Westbury, NY) by centrifugation at 95,000 rpm for 5 min at 4°C with an RP100AT3 rotor in a Sorvall RC M100 microultracentrifuge. Cytosolic fractions were prepared by centrifugation of PNS at 95,000 rpm for 15 min at 4°C using an RP100AT2 rotor in the same instrument. For some experiments, cytosol was also desalted on 1 ml G-25 Sephadex spin columns equilibrated with breaking buffer.

In vitro activity supporting vesicle fusion with a common compartment, which results in AvβGal:B-Tf complex formation, was assayed by co-incubation of 5 μl aliquots of PNS or separated vesicle fractions containing AvβGal and B-Tf in 50 μl breaking buffer supplemented with 1 mM MgATP, 100 μg/ml creatine kinase, 8 mM phosphocreatine, 10 μg/ml biotin-cytochrome C, and 1 mM dithiothreitol at 37°C for 30 min. The fusion reaction was terminated by addition of 5 μl lysis buffer (10% Triton X-100, 1% SDS, 50 μg/ml biotin-cytochrome C) and 200 μl dilution buffer (0.05% Triton X-100, 50 mM NaCl, 10 mM Tris, pH 7.4, 1 mg/ml heparin); lysates were clarified by centrifugation at 14,000 rpm for 5 min at 4°C in a Eppendorf microcentrifuge. The complex between AvβGal and B-Tf resulting from their colocalization was measured by a modified enzyme-linked immunoabsorbent assay (Braell, 1987). Briefly, the AvβGal:B-Tf complex was captured by incubation of clarified lysates in microtiter wells coated with rabbit anti-Tf antibodies. After

extensive washing, AvβGal activity associated with the wells was determined by measuring the hydrolysis of the fluorogenic substrate 4-methylumbelliferyl β-galactoside. The fluorescence of the hydrolyzed product was measured using an Hitachi F-2000 spectrophotometer. Background activity measured at 4°C is subtracted from these values to determine specific complex formation due to endosome fusion events.

## Fluorescence and Indirect Immunofluorescence Microscopy

HeLa cells were grown on glass coverslips (12 mm/diameter in 24-well plates) to approximately 50% confluence in α-MEM containing 10% fetal bovine serum. Before experiments, cells were incubated for 4 h in serum-free α-MEM containing 1 mg/ml BSA, and subsequently rinsed twice in KRH buffer (25 mM HEPES-NaOH, pH 7.48, 120 mM NaCl, 6 mM KCl, 1.2 mM $MgCl_2$, 1 mM $CaCl_2$, 1.8 mg/ml glucose, 1 mg/ml BSA). KRH buffer, containing either 100 nM wortmannin (a 1:1000 dilution from a 100 $\mu$M stock in DMSO) or DMSO alone, was added to the cells for 60 min at 37°C. After this time, fresh media containing 20 nM Texas Red-Tf was added and incubation was continued for 45 min at 37°C. Tf uptake was stopped by placing the 24-well plates on ice followed by several washes with chilled PBS containing 1 mM $MgCl_2$ and 0.1 mM $CaCl_2$; cells were subsequently fixed with 3% paraformaldehyde in the same buffer for 30 min at room temperature. The coverslips were then transferred to a humidified chamber and incubated for 30 min at room temperature with 25 $\mu$l PBS containing 1 mM $MgCl_2$, 0.1 mM $CaCl_2$, 1 mg/ml BSA, 0.02% saponin, and either antibody to the TfR (1:500 dilution), antibody to the $\gamma$ subunit of AP-1 (1:1 dilution), anti-LAMP-1 antibody (1:10 dilution), or anti-M6PR antibody (1:1000 dilution). After rinsing, the cells were covered with 25 $\mu$l PBS containing 1 mM $MgCl_2$, 0.1 mM $CaCl_2$, 1 mg/ml BSA, 0.02% saponin, and secondary anti-mouse IgG-FITC antibody (1:100 dilution). After incubation for 30 min at room temperature, coverslips were extensively rinsed and mounted onto glass slides, with the cells immersed in PBS containing 1 mM $MgCl_2$, 0.1 mM $CaCl_2$, 80% glycerol, and 2 mg/ml p-phenylenediamine. Immunofluoresence microscopy was carried out with a Zeiss Axioskop epifluorescence microscope (Thornwood, NY) at a nominal magnification of 100×.

## RESULTS

### Wortmannin Down-Regulates Surface TfRs

To determine the effects of wortmannin on steady-state cell surface TfR number, binding of radiolabeled ligand was measured for K562 cells treated with or without 100 nM wortmannin for 60 min. Scatchard plots of ^{125}I-Tf binding demonstrate that although the dissociation constant ($K_d$) for ligand binding to the TfR is unaltered, wortmannin promotes a significant decrease (31 ± 2%; n = 3) in the number of surface binding sites (Bmax) (Figure 1A). Wortmannin is potent in its effects ($IC_{50}$ ~25 nM; Figure 1B) and acts rapidly with maximal effects observed within 30 min of exposure to the drug (Figure 1C). Although it is possible that the loss of surface TfRs might be due to missorting to lysosomes or to mislocalization of lysosomal hydrolases to TfR-containing endosomes, control experiments confirmed that the total number of cellular Tf binding sites is the same for wortmannin-treated and control cells. Thus, the decrease in cell surface receptor number does not reflect receptor degradation.

Down-regulation of surface TfRs could result from either an increase in the rate of endocytosis or a decrease in the rate of exocytosis. To investigate the effects of wortmannin on endocytosis, uptake of ^{125}I-Tf by K562 cells at 37°C was measured. IN/SUR was plotted as a function of time to determine $k_e$, the endocytic rate constant, from the initial slope of this line (Wiley and Cunningham, 1982). As shown by the results of Figure 2A, wortmannin promotes an ~1.6-fold increase in $k_e$. Values for $k_e$ were determined to be 0.160 ± 0.02 and 0.260 ± 0.07 $\text{min}^{-1}$ for control and wortmannin-treated K562 cells, respectively (n = 5).

To study the kinetics of TfR exocytosis, K562 cells were loaded with ^{125}I-Tf for 1 h at 37°C in the presence or absence of 100 nM wortmannin, washed free of external and surface-bound ligand, and then release of internalized ligand at 37°C was monitored in the continued presence or absence of wortmannin. Under these conditions, wortmannin decreases the rate of TfR recycling (Figure 2B). Previous studies have documented that exocytosis of Tf from K562 cells is biphasic, suggesting that release occurs from two internal pools of recycling ligand (Snider and Rogers, 1985; Stein and Sussman, 1986; Schonhorn and Wessling-Resnick, 1994). Analysis of data from three independent experiments indicates that wortmannin alters the kinetic rate constants determined for Tf exocytosis from both compartments (Table 1). Thus, TfR down-regulation is induced by wortmannin's dual actions to stimulate endocytosis and to decrease exocytosis of recycling receptors.

### Wortmannin Inhibits Colocalization of Endocytic Probes In Vitro

To investigate how wortmannin might act on intermediate steps in the TfR recycling pathway, we examined its effects in a cell-free assay that reconstitutes stages of endosome-endosome fusion, receptor sorting, and/or trafficking to the sorting endosome (Wessling-Resnick and Braell, 1990). Briefly, PNS fractions containing endocytic vesicles and endosomes loaded with AvβGal or B-Tf are incubated at 37°C in the presence of ATP; fusion events resulting in the colocalization of the two probes can be detected due to AvβGal:B-Tf complex formation due to avidin-biotin association.

An example of a typical experiment following the timecourse of AvβGal:B-Tf complex formation is shown in Figure 3A. The presence of 100 nM wortmannin causes a 40% decrease in fusion activity within 20 min of the in vitro reaction. This observation indicates that the arrival of B-Tf to an AvβGal-positive compartment is blocked. The rate of the in vitro fusion reaction is also reduced approximately threefold. The inhibitory action of wortmannin is induced within 15 min of incubation of the vesicle fractions on ice; control experiments demonstrated that exposure of sam-
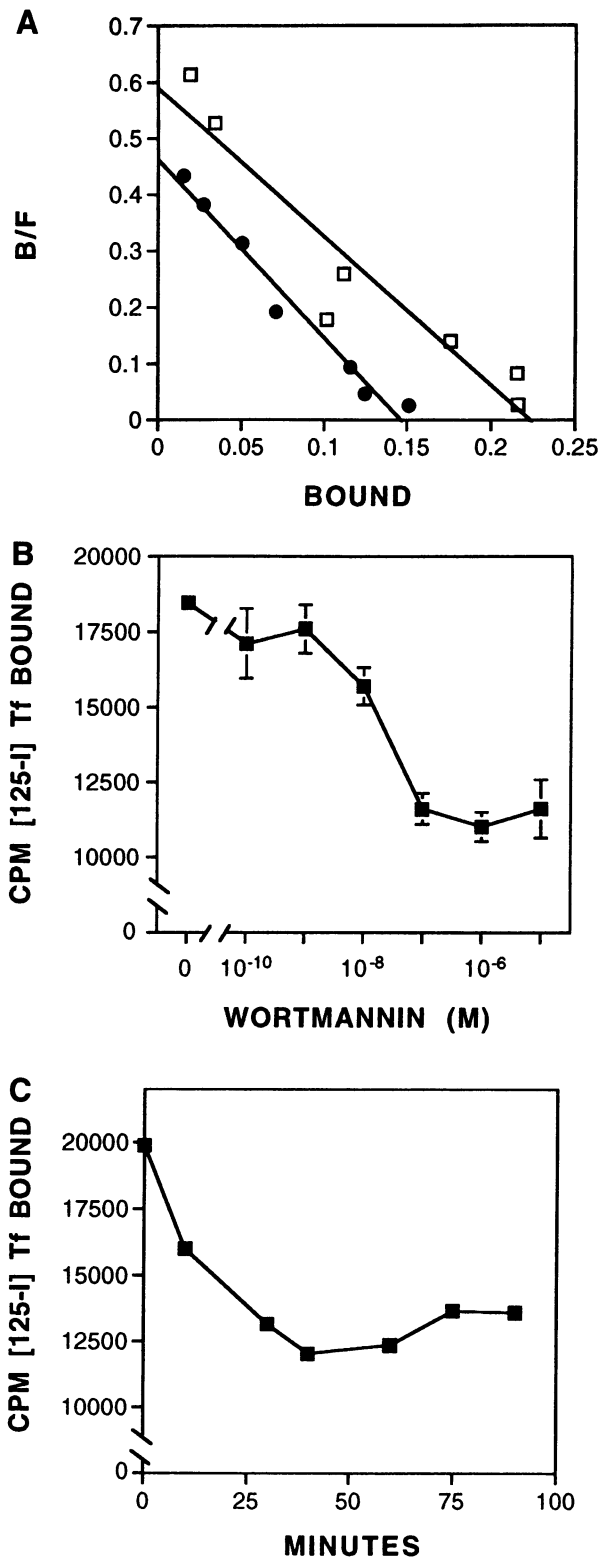
ples to the drug for up to 60 min did not result in further loss of signal. The dose response of the in vitro assay reveals an $IC_{50}$ ~15 nM wortmannin (Figure 3B); this value is comparable to the concentration of wortmannin found to induce half-maximal down-regulation of the TfR in vivo (Figure 1C). However, a small amount of probe colocalization persists even at wortmannin concentrations above 1 $\mu$M, suggesting that a subpopulation of endosomes are resistant to wortmannin's effect.

To determine whether wortmannin inhibits a membrane-associated or cytosolic factor, vesicle fractions and cytosol were separately incubated with or without wortmannin and then recombined in the in vitro assay with the results shown in Figure 4A. As expected, maximum colocalization of the endocytic probes is recovered with untreated membranes and cytosol; fusion activity is stimulated four- to fivefold relative to that measured in the absence of cytosol. This activity is not inhibited in assays containing untreated vesicles in the presence of wortmannin-treated cytosol. Moreover, only a minor loss of activity is detected when wortmannin-treated vesicles are assayed in the presence of untreated cytosol. Since wortmannin treatment of both fractions results in ~70% inhibition, we conclude that the wortmannin-sensitive factor is present in both membrane-associated and soluble pools and that it is necessary to inactivate activity in both fractions to block the cell-free assay. A second conclusion is that the wortmannin-sensitive activity associated with the vesicle population is sufficient to support membrane trafficking events in the cell-free assay because wortmannin treatment of cytosol alone is without effect.

The data of Figure 4A also demonstrate that wortmannin inhibition of membrane-associated factors can

Figure 1. Wortmannin down-regulates K562 cell surface TfRs. (A) Scatchard analysis of ^{125}I-Tf binding. K562 cells were incubated at 4°C in the absence or presence of 100 nM wortmannin for 60 min at 37°C. After several washes in PBS, binding assays containing 10[6]

(Figure 1 cont.) cells with 0.5–50 nM ^{125}I-Tf in the presence or absence of 5 $\mu$M unlabeled Tf were incubated at 4°C for 60 min. Specific cell-associated radioactivity (B) and unbound ligand (F) were measured as described in MATERIALS AND METHODS. Scatchard analysis was employed to determine the number of Tf-binding sites (Bmax) and the dissociation constant ($K_d$). Bmax values of 2.66 × 10^{5} and 1.26 × 10^{5} TfRs/cell and $K_d$ values of 1.52 nM and 1.27 nM were found for control (open squares) and wortmannin-treated (closed circles) cells, respectively. Data are from a single experiment and are representative of three independent experiments. (B) Dose response to wortmannin. K562 cells were treated with the indicated concentrations of wortmannin for 60 min at 37°C. Specific binding was measured in assays containing 10[6] cells incubated with 25 nM ^{125}I-Tf in the presence or absence of excess cold ligand at 4°C. Data points represent the mean of triplicate samples (± SD). Similar results were obtained on three separate occasions. (C) Time-course of TfR down-regulation. K562 cells were incubated at 37°C with 90 nM wortmannin; at the times indicated, 10[6] cells were withdrawn, washed, and resuspended in binding assays containing 10 nM ^{125}I-Tf with or without 5 $\mu$M unlabeled ligand. Specific ^{125}I-Tf binding was then determined at 4°C; the cpm measured for cell-associated ^{125}I-Tf is shown as a function of time of incubation with wortmannin.
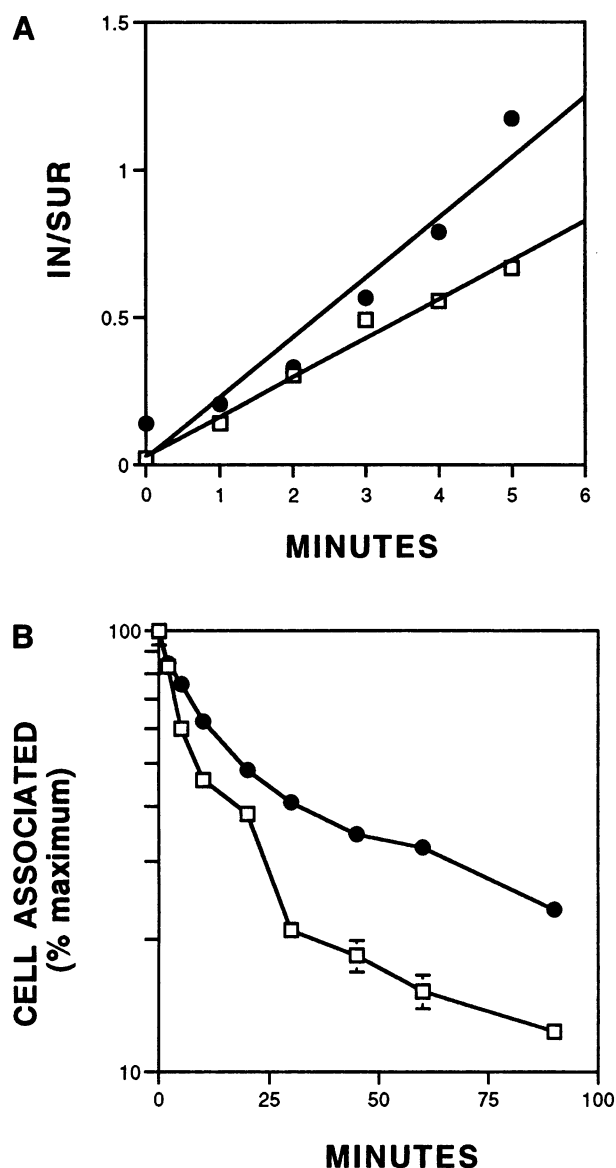
**A**



**B**



**Figure 2.** Effects of wortmannin on Tf endocytosis and exocytosis. (A) IN/SUR analysis. K562 cells were incubated for 40 min at 37°C with (filled circles) or without (open squares) 100 nM wortmannin and washed three times in PBS. Aliquots of $10^6$ cells were then incubated at 37°C in the presence of 25 nM radiolabeled Tf for the times indicated. The amounts of total, internalized (IN), and surface-associated (SUR) radiolabel were determined as described in MATERIALS AND METHODS. Data are plotted according to the IN/SUR method of Wiley and Cunningham (1982) wherein the slope is equal to the endocytic rate constant $k_e$. Shown are results from a single experiment and are representative of those obtained on five separate occasions. (B) Wortmannin reduces Tf recycling. K562 cells were incubated at 37°C in the presence of 25 nM ^{125}I-Tf in the absence (open squares) or presence (filled circles) of 100 nM wortmannin for 1 h. Cells were then pelleted, washed, stripped of surface label, and release of internalized radiolabel was monitored at 37°C in the presence of 250 nM unlabeled Tf. Shown is the semi-log plot of the percent of initial cell-associated ^{125}I-Tf remaining as a function of time. Data are the means of duplicate samples and are representative of three independent experiments.

**Table 1.** Kinetic parameters of transferrin exocytosis in K562 cells

| | Rate constant (min$^{-1}$) | |
| --- | --- | --- |
| | $k_f$ | $k_s$ |
| Control | 0.2018±0.0433 | 0.0169±0.0069 |
| Wortmannin | 0.1542±0.0429 | 0.0096±0.0045 |

Release of ^{125}I-Tf was performed as described for Figure 2B and in MATERIALS AND METHODS. Assuming that the ligand recycles from two separate noninteracting compartments, the data best fit the equation $y = a_f e^{k_f t} + a_s e^{k_s t}$; where $k_f$ and $k_s$ are the "fast" and "slow" rate constants, respectively (Schonhorn and Wessling-Resnick, 1994). Shown are the mean ± SD determined in three separate experiments.

be reversed by the addition of untreated cytosol, further suggesting that recruitment of wortmannin-sensitive components onto the surface of vesicles is a necessary step for membrane traffic events. This idea is supported by the results of Figure 4B, which demonstrate the concentration-dependent ability of untreated cytosol to restore activity to wortmannin-treated vesicles in the cell-free assay. Thus, cytosolic wortmannin-sensitive factors can cycle on and off membranes to engage in the TfR's endocytic pathway but they appear to exert their functional effects at the endocytic vesicle surface.

## Wortmannin Selectively Disrupts Endosomal Compartments

To characterize wortmannin's effect on the morphology of endosomes, HeLa cells were utilized because the adherent growth of this cell line facilitates the use of fluorescence microscopy. Figure 5 shows the typical intracellular distribution of Texas Red-Tf after a 45 min internalization period (Figure 5A). Structures containing Tf are vesicular in appearance and abundant throughout the cytoplasm with a more concentrated signal in the perinuclear region of the cell. Incubation with wortmannin induces dramatic changes in the morphology of the Tf-containing structures (Figure 5B). Cytoplasmic vesicles appear swollen and enlarged and the perinuclear endosomal compartment also appears disrupted and expanded with the formation of highly condensed areas of Tf staining. To verify that wortmannin does not cause dissociation of Tf from the TfR, TfR distribution was compared by indirect immunofluorescence and found to completely overlap with Texas Red-Tf fluorescence (Figure 5C, compare arrowheads with Figure 5B). Therefore, in the experiments described below, Texas Red-Tf staining identifies the intracellular distribution of endocytosed TfRs.

The structure of the trans-Golgi network (TGN) was evaluated in control and wortmannin-treated

cells by examining staining profiles of the γ-subunit of the clathrin-associated AP-1 complex. Figure 6A confirms the intense juxtanuclear staining of the γ-subunit due to association of AP-1 complexes with the TGN (Ahle et al., 1988). As has been previously reported (Robinson and Kreis, 1992), immunofluorescent staining of AP-1 γ-subunit is also observed throughout the periphery of the cell in punctate vesicular structures. Wortmannin treatment does not cause a redistribution of juxtanuclear AP-1 fluorescence, but does cause an overall retraction of the γ-subunit staining from the cell's periphery (Figure 6B).

Cells were also counterstained with antibodies to the lysosomally associated protein LAMP-1. Figure 7 shows the typical profiles of endocytosed Tf (Figure 7A) and LAMP-1 (Figure 7B), demonstrating that the distribution of these two proteins is distinct. LAMP-1 staining is not significantly affected by wortmannin (Figure 7D) and does not appear to colocalize in the swollen peripheral endosomes containing Tf (Figure 7C).

The distribution of a late endosomal marker, the M6PR, is perturbed by wortmannin as previously reported (Brown et al., 1995). In control cells, M6PR immunofluorescence is highly concentrated in perinuclear structures restricted to a defined segment of the nuclear circumference, although discrete vesicular elements are also observed in the peripheral cytoplasm (Figure 8B). Although some of the Tf and M6PR fluorescence overlaps, a significant fraction of the peripheral Tf-labeled endosomes do not contain any M6PR signal. Wortmannin fragments the highly concentrated juxtanuclear M6PR signal, with staining observed in swollen vesicular elements distributed over the entire nuclear circumference (Figure 8D). Similar observations were reported by Brown et al. (1995) for rat clone 9 hepatocytes treated with similar concentrations of wortmannin. However, the majority of swollen, dilated Tf-containing endosomes remain distinct from M6PR-positive structures.

## DISCUSSION

Our investigation characterizes pleiotropic effects of wortmannin on the TfR's endocytic pathway in vivo and in vitro including the following: 1) the rapid down-regulation of ~30% of K562 cell surface TfRs, 2) an induced increase in the endocytic rate constant, 3) a reduction in the rate of TfR exocytosis, and 4) potent inhibition of colocalization between endocytosed B-Tf and AvβGal in vitro. These differential effects indicate that wortmannin can perturb membrane traffic of the TfR at multiple steps; for example, increased endocytosis and decreased exocytosis both contribute to the down-regulation of surface receptors. Wortmannin also induces dramatic alterations in the morphology of
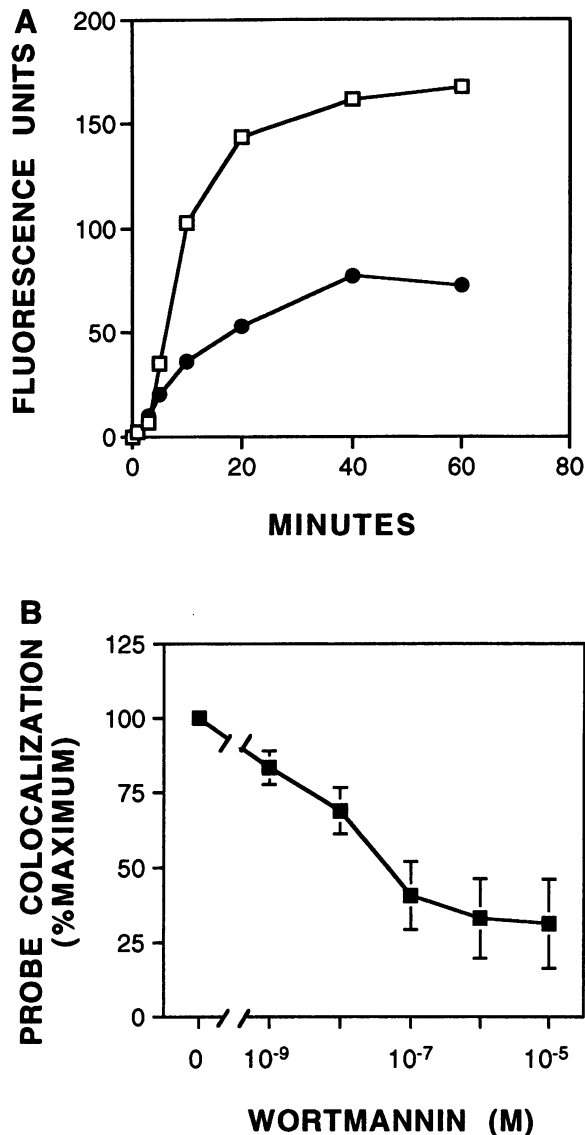
Figure 3. Wortmannin inhibits endocytic vesicle fusion. (A) Time course of endocytic probe colocalization. K562 PNS and cytosol containing endocytosed AvβGal and B-Tf probes were independently incubated on ice with (closed circles) or without (open squares) 100 nM wortmannin. PNS and cytosol were then added to fusion reaction mixtures containing ATP and an ATP-regenerating system and incubated at 37°C for the indicated times. Colocalization of the probes due to vesicle fusion with a common compartment is detected by measuring B-Tf-associated βGal activity with a fluorescent substrate. Details of this assay may be found in MATERIALS AND METHODS. Shown is the time course of probe colocalization (measured in fluorescence units). The initial rates for control and wortmannin-treated samples were determined to be 12.6 and 4.5 fluorescence units·min$^{-1}$, respectively. Data are representative of results obtained in three independent experiments. (B) Dose response to wortmannin. PNS and cytosol fractions were preincubated on ice in the presence of the indicated concentrations of wortmannin; in vitro assays were then performed as described above, with incubation of the reaction mixtures at 37°C for 30 min. Data points are the mean values of the percentage of maximal activity determined in five independent experiments (± SD).

**A**



VESICLES     −     −     +     +

CYTOSOL    −     +     −     +

**B**



**CYTOSOL (mg/ml)**

Tf-containing endocytic compartments in HeLa cells and appears to target elements of the endocytic pathway as noted by changes in the profile of TfR- and M6PR-containing structures corresponding to early and late endosomal compartments, respectively.

The observed effects of wortmannin on the cell surface TfR number and endosomal morphology resemble its action on M6PR distribution as reported by Brown *et al.* (1995). These investigators observed a down-regulation of surface M6PRs and an increase in TGN-associated receptors over time. It should be noted that in the latter study, the formation of enlarged phase-luscent organelles was observed to be induced by wortmannin. Under the conditions of our study, such vacuoles are not observed. This difference in results could be due either to the lower concentrations of wortmannin used in our experiments (nM versus $\mu$M levels) or because the concentration of wortmannin required to elicit effects varies from cell-type to cell-type (Davidson, 1995). The fact that early and late endosomal compartments are both affected suggests that wortmannin may interfere with a regulatory step common to both the TfR and M6PR pathways.

Observations drawn from our in vitro experiments may offer some molecular insights into the nature of wortmannin's effects on receptor recycling. We speculate that inhibition of Av$\beta$Gal and B-Tf colocalization results from the failure to form cargo vesicles de novo in the presence of the drug. Endocytic probes internalized independently of one another are known to mix in a common endosomal compartment in vivo and in vitro (Braell, 1987; Salzman and Maxfield, 1988; Gruenberg *et al.*, 1989; Wessling-Resnick and Braell, 1990). However, there is debate as to whether the transfer of material between endosomal compartments occurs via maturation of these domains (Murphy, 1991) or through vesicular transport between stable pre-existing organelles (Griffiths and Gruenberg, 1991). Thus, colocalization of endocytic probes detected by the in vitro fusion assay could occur through direct fusion of pre-exisiting endosomes or through mixing of the probes after a cycle of sorting, vesicle formation, and the subsequent fusion of budded vesicles to a common compartment. Because the in vitro effects of wortmannin are characterized by the
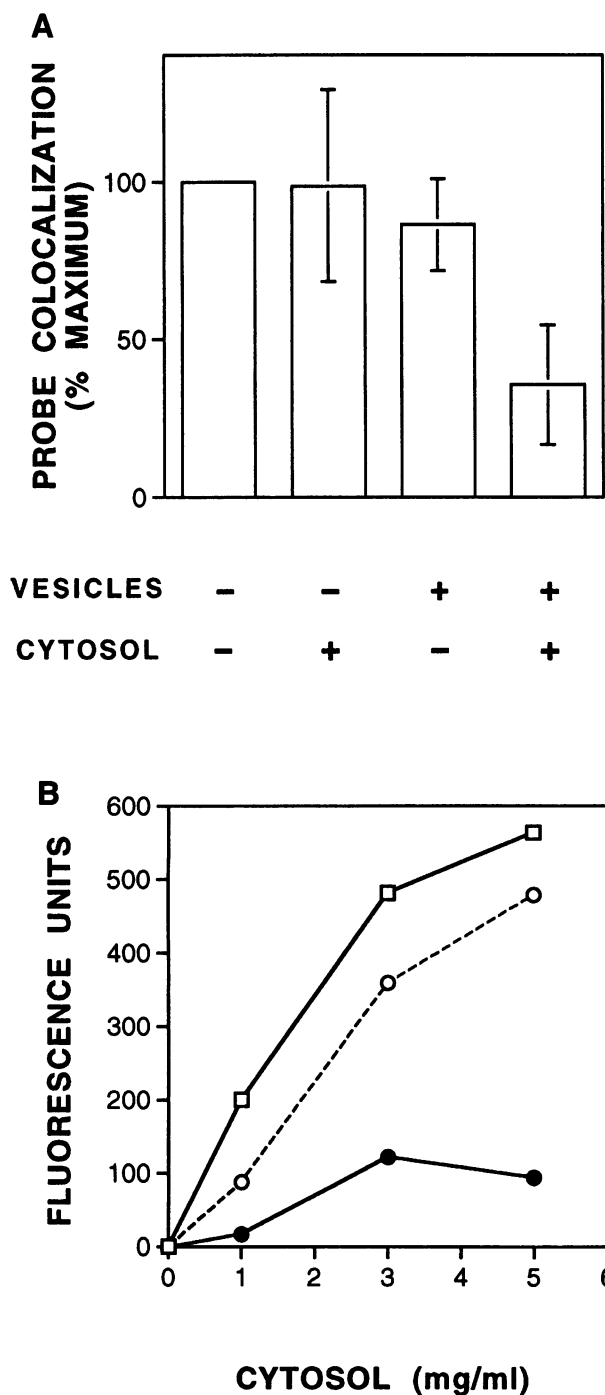
**Figure 4.** Effects of wortmannin on cytosolic and membrane fractions. (A) Wortmannin inhibits cytosolic and membrane-associated factors. PNS and cytosol were incubated in the absence (−) or presence (+) of 100 nM wortmannin. To remove residual wortmannin, vesicle fractions were separated using a Nycodenz step gradient and cytosol was gel filtered over G-25 spin columns. These fractions were then mixed in fusion assays in the combinations indicated; incubation of assay mixtures was at 37°C for 30 min. Data points are the mean values of the percentage of maximal activity determined in four independent experiments (± SD). (B) Cytosol restores in vitro activity to wortmannin-treated membranes in a

(**Figure 4 cont.**) dose-dependent manner. PNS and cytosol were incubated with or without wortmannin as described for panel A. Gel-filtered cytosol was then combined in fusion assays with separated vesicle fractions at the final concentrations indicated; incubation of reaction mixtures was at 37°C for 30 min. Data are from a single experiment with similar results obtained on three separate occasions. Results are shown for the following: untreated membranes and cytosol (open squares), wortmannin-treated membranes and untreated cytosol (open circles), and wortmannin-treated membranes and cytosol (closed circles).
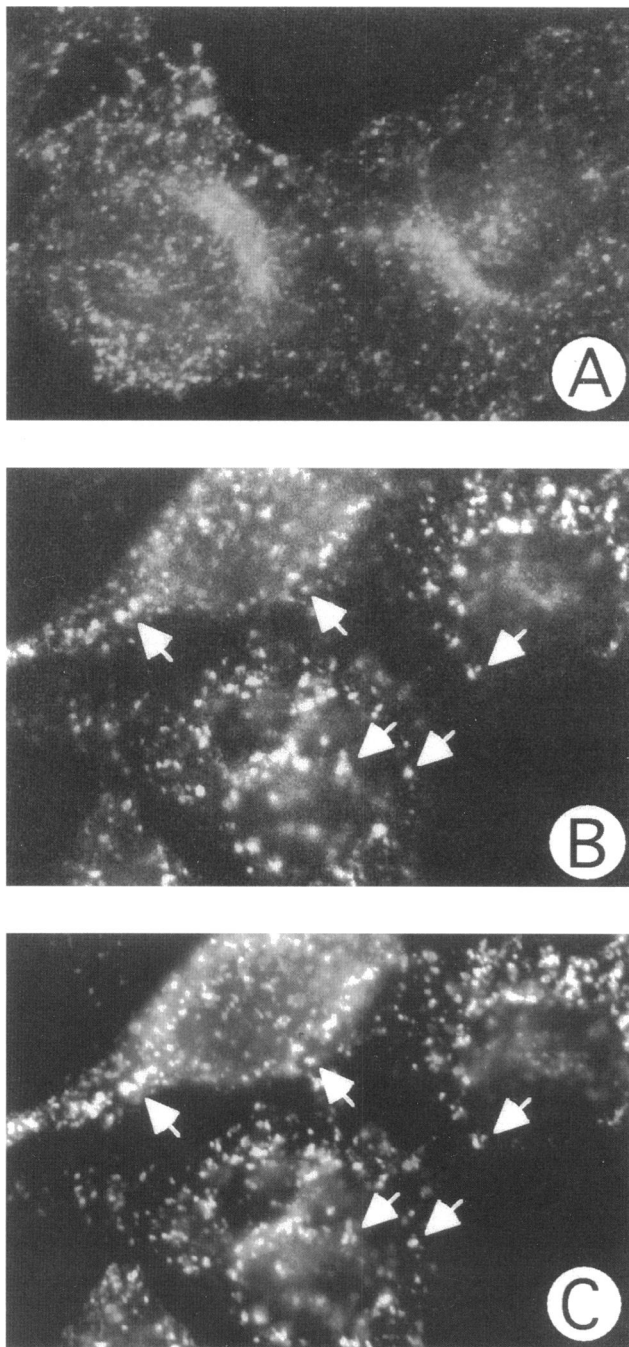
recruitment of a wortmannin-sensitive cytosolic factor onto the surface of membranes, we favor the latter view. The idea that wortmannin interferes with TfR sorting and vesicle budding is consistent with the activity of the *VPS34* gene product, which is known to block traffic from the yeast Golgi at a late sorting step (Schu *et al.*, 1993) and to regulate endosomal sorting mechanisms (Munn and Riezmann, 1994). A consequence of the hypothetical inhibition of vesicle budding would be enlarged, swollen, or dilated endosomes, a prediction borne out by the morphology observed in wortmannin-treated cells. A second prediction is that failure to sort the Tf-TfR complex would retard its progress through the exocytic pathway; in fact, a reduced rate of receptor recycling is observed in vivo. Although the proposal that wortmannin disrupts intracellular receptor sorting and vesicle budding is consistent with several of the effects we observe in vivo, the enhanced rate of TfR internalization
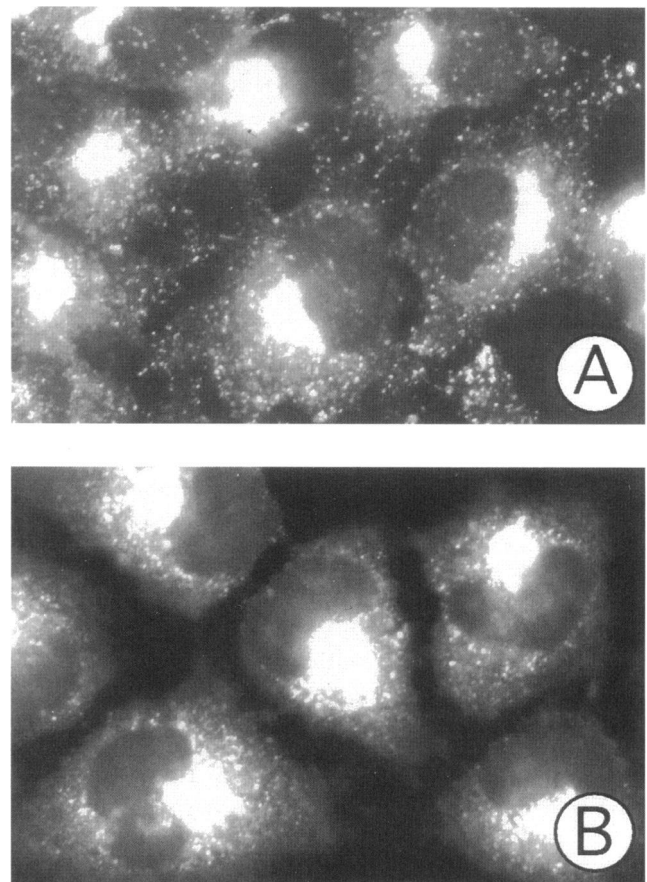


**Figure 5.** Wortmannin perturbs morphology of Tf-containing compartments in HeLa cells. HeLa cells were treated in the absence (A) or presence (B and C) of 100 nM wortmannin for 60 min at 37°C. To visualize endosomal compartments, incubation was continued for an additional 45 min in the presence of 20 nM Texas Red-Tf. Cells were fixed, permeabilized, and stained with antibodies to the human transferrin receptor; primary antibody was visualized with fluorescein-conjugated anti-rabbit IgG. (A and B) Texas Red-Tf; (C) staining profiles for the human transferrin receptor. Arrowheads in panels B and C show overlap of Tf and TfR.



**Figure 6.** Wortmannin effect on AP-1 distribution. HeLa cells were treated in the absence (A) or presence (B) of 100 nM wortmannin for 60 min at 37°C. Cells were fixed, permeabilized, and stained with antibodies to the γ-subunit of the clathrin-associated complex AP-1; primary antibody was visualized with fluorescein-conjugated anti-rabbit IgG.
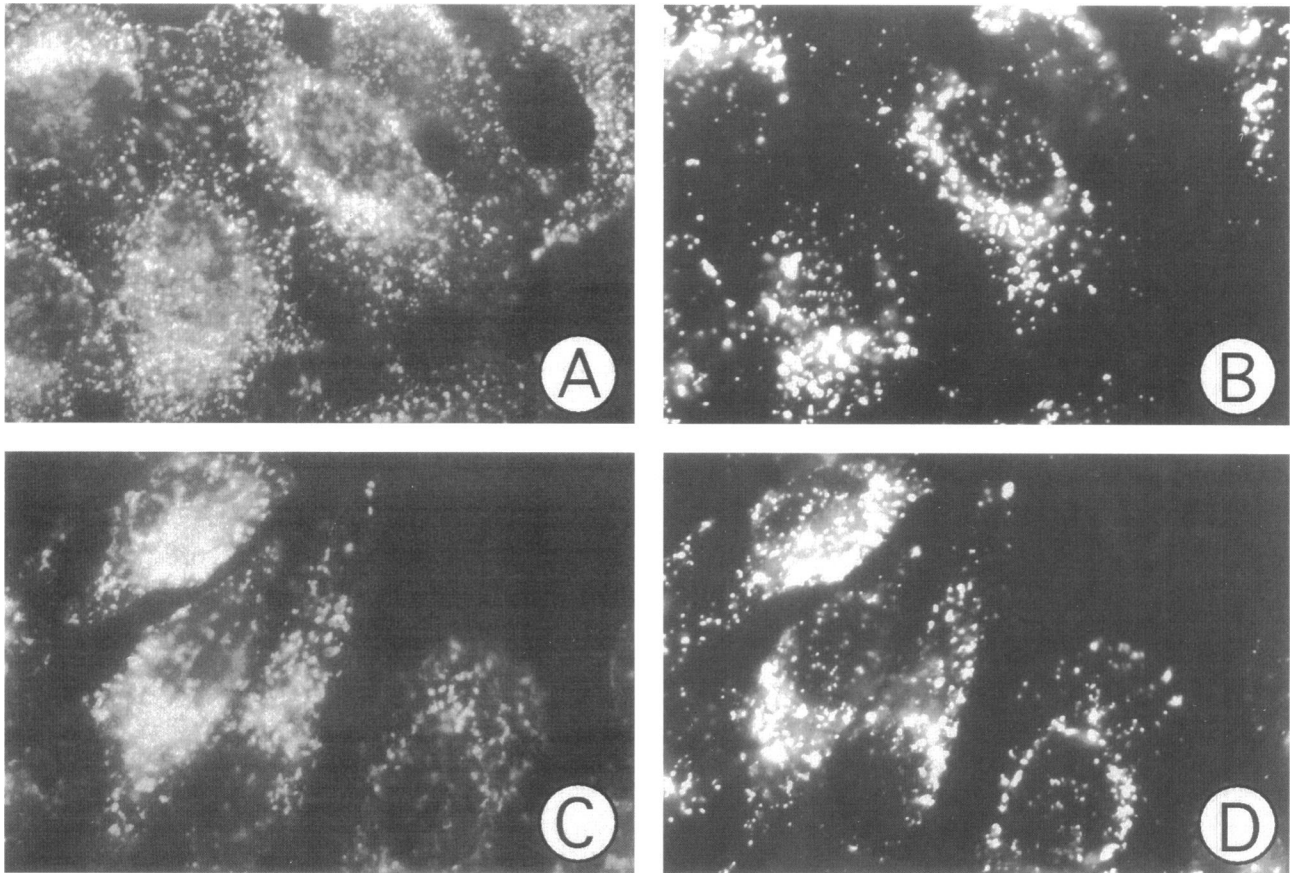
**Figure 7.** LAMP-1 distribution in wortmannin-treated HeLa cells. HeLa cells were treated in the absence (A and B) or presence (C and D) of 100 nM wortmannin and allowed to internalize Texas Red-Tf as described in Figure 5. To cytolocalize lysosomes, cells were fixed, permeabilized, and incubated with anti-LAMP-1, followed by FITC-conjugated anti-mouse IgG to visualize primary antibody. (A and C) Texas Red-Tf; (B and D) staining profiles for LAMP-1.

suggests that early stages of receptor sorting in the endocytic pathway are differentially regulated.

The fact that wortmannin is known to act on multiple protein targets might explain its differential effects on the TfR pathway. For example, recent work has demonstrated that several PI 3-kinase isoforms exist in mammalian cells. The best characterized activity is the p85/110 complex (Carpenter *et al.*, 1990). A second PI 3-kinase isotype, p110γ, fails to associate with the regulatory p85 subunit, but can be activated by heterotrimeric G protein subunits (Stephens *et al.*, 1994; Stoyanov *et al.*, 1995). Both of these PI 3-kinases are inhibited by wortmannin in the nM range. A newly discovered mammalian homologue of the yeast PI-specific PI 3-kinase vps34 is also inhibited by low nM levels of wortmannin (Volinia *et al.*, 1995). Thus, the observations that at least two independent stages of TfR traffic are differentially affected by wortmannin (i.e., increased internalization from the plasma membrane and inhibition of delivery into "mixing" endosomes), may suggest that multiple PI 3-kinase iso-

forms function in recognition and sorting of the receptor from distinct membrane domains. However, it is also important to note that the effects of wortmannin are not restricted to PI 3-kinases; a PI 4-kinase sensitive to nM levels of the inhibitor has been characterized (Nakanishi *et al.*, 1995). Both PI 4-kinases and PI 4-P 5-kinases have been implicated in vesicle traffic. PI 4-kinase activity is associated with glucose transporter-containing vesicles that are recruited to the plasma membrane in response to insulin (Del Vecchio *et al.*, 1991). A PI 4-P 5-kinase has been purified based on its activity to support fusion of secretory granules with the plasma membrane (Hay *et al.*, 1995). Yeast *FAB1* mutants also have revealed that PI 4-P 5-kinase activity is important to maintain vacuolar function (Yamamoto *et al.*, 1995). Since PI transfer proteins, which function to present PI to inositol kinases, are implicated in the formation of secretory vesicles from the TGN (Ohashi *et al.* 1995) and in priming secretory vesicles for fusion with the plasma membrane (Hay *et al.*, 1995), evidence for a general role for phosphory-
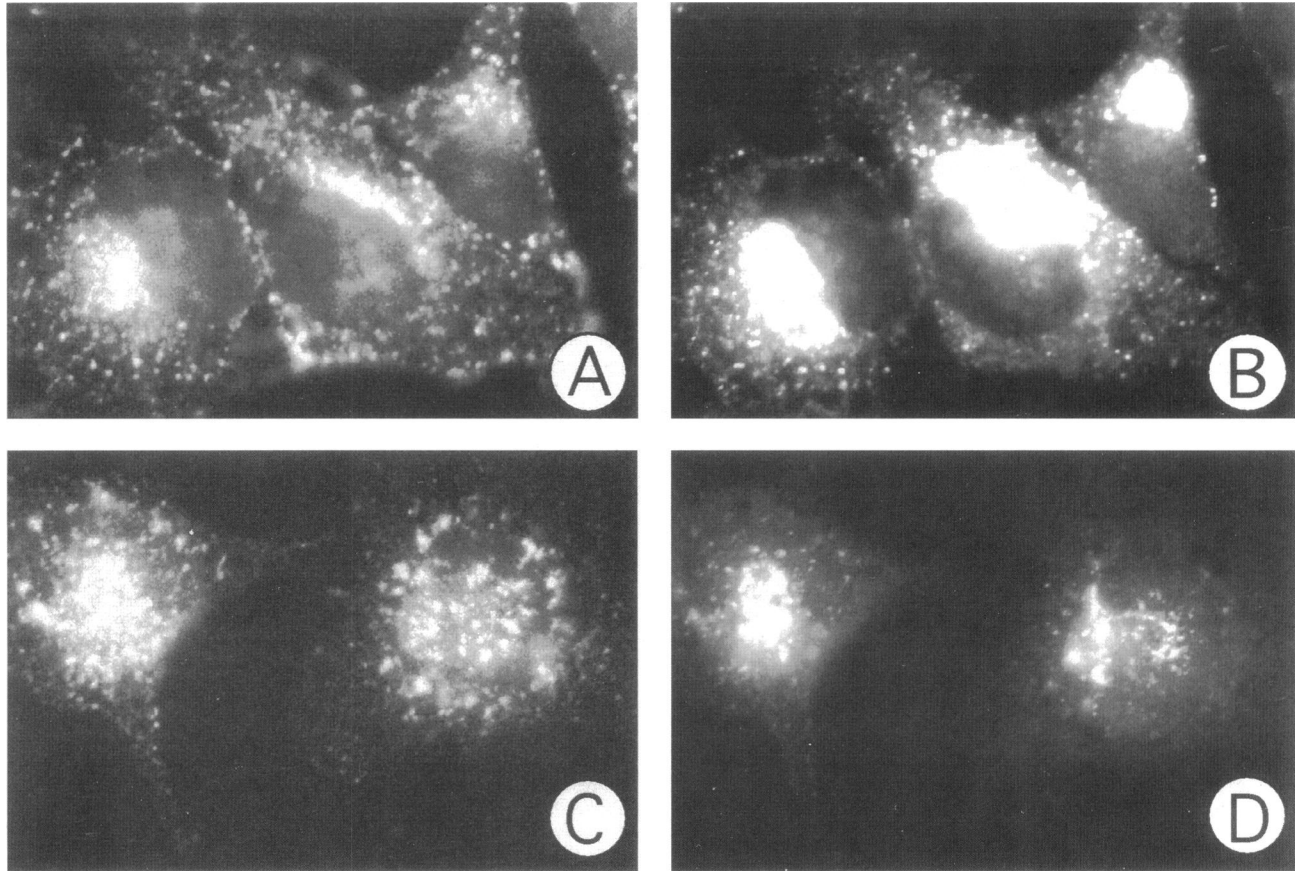
**Figure 8.** Wortmannin effects on M6PR distribution in HeLa cells. HeLa cells were incubated without (A and B) or with (C and D) 100 nM wortmannin and allowed to internalize Texas Red-Tf. Cells were then fixed, permeabilized, and incubated with monoclonal anti-M6PR, and subsequently incubated with FITC-conjugated anti-mouse IgG to visualize primary antibody. (A and C) Texas Red-Tf; (B and D) staining profiles for M6PR.

lated PI lipids in different steps of membrane traffic exists. Further investigation is required to establish the precise targets through which wortmannin's effects on TfR membrane traffic are mediated. Results of these future studies may help to resolve issues surrounding the nature of organelles comprising the endocytic pathway.

**Note Added in Revision.** While this article was under review, Li *et al.* (1995) reported that wortmannin treatment of TRVb-1 cells *decreases* TfR endocytosis as well as slowing exocytosis. Wortmannin was also found to inhibit fusion of endosomes derived from BHK cells (Jones and Clague, 1995) and J774E macrophages (Li *et al.*, 1995). In the latter study, addition of activated p85/110 PI-3 kinase increased endosome fusion. Although these data support a role for PI 3-kinase in endosome-endosome fusion, it cannot be concluded that the effects of wortmannin on endosome fusion in vitro are due to specific inhibition of the p85/110 kinase. In this regard, Cross *et al.* (1995) also have recently reported that wortmannin inhibits bombesin-

stimulated phospholipase $A_2$ ($IC_{50}$ ~2 nM); a previous study indicated that inhibitors of phospholipase $A_2$ activity block fusion of J774E endosomes in vitro (Mayorga *et al.*, 1993). In fact, addition of purified p85/110 kinase (kindly provided by Drs. L.C. Cantley and C.L. Carpenter) did not reverse the inhibition of in vitro fusion by wortmannin in our hands, similar to observations reported by Jones and Clague (1995).

## ACKNOWLEDGMENTS

## REFERENCES

Acaro, A., and Wymann, M.P. (1993). Wortmannin is a potent phosphatidyl 3-kinase inhibitor: the role of phosphatidyl 3,4,5-triphosphate in neutrophil responses. Biochem. J. *296*, 297–301.

Ahle, S., Mann, A., Eichelsbacher, U., and Ungewickell, E. (1988). Structural relationships between clathrin assembly proteins from the Golgi and the plasma membrane. EMBO J. 7, 919–929.

Braell, W.A. (1987). Fusion between endocytic vesicles in a cell-free system. Proc. Natl. Acad. Sci. USA 84, 1137–1141.

Brown, W.J., DeWald, D.B., Emr, S.D., Plutner, H., and Balch, W.B. (1995). Role for phosphatidylinositol 3-kinase in the sorting and transport of newly synthesized lysosomal enzymes in mammalian cells. J. Cell. Biol. 130, 781–796.

Carpenter, C.L., Duckworth, B.C., Auger, K.R., Cohen, B., Schaffhausen, B., and Cantley, L.C. (1990). Purification and characterization of phosphoinositide 3-kinase from rat liver. J. Biol. Chem. 265, 19704–19711.

Clague, M.J., Thorpe, C., and Jones, A.T. (1995). Phosphatidylinositol 3-kinase regulation of fluid phase endocytosis. FEBS Lett. 367, 272–274.

Clark, J.F., Young, P.W., Yonezawa, K., Kasuga, M., and Holman, G.D. (1994). Inhibition of the translocation of GLUT1 and GLUT4 in 3T3-L1 cells by the phosphatidylinositol 3-kinase inhibitor, wortmannin. Biochem. J. 300, 631–635.

Cross, M.J., Stewart, A., Hodgkin, M.N., Kerr, D.J., and Wakelam, M.J.O. (1995). Wortmannin and its structural analogue demethoxyviridin inhibit stimulated phospholipase A2 activity in Swiss 3T3 cells. J. Biol. Chem. 270, 25352–25355.

Dautry-Varsat, A., Ciechanover, A., and Lodish, H.F. (1983). pH and the recycling of transferrin during receptor-mediated endocytosis. Proc. Natl. Acad. Sci. USA 80, 2258–2262.

Davidson, H.W. (1995). Wortmannin causes mistargeting of procathepsin D: evidence for the involvement of a phosphatidylinositol 3-kinase in vesicular transport to lysosomes. J. Cell. Biol. 130, 797–805.

Del Vecchio, R.L., and Pilch, P.F. (1991). Phosphatidyl 4-kinase is a component of glucose transporter (GLUT 4)-containing vesicles. J. Biol. Chem. 266, 13278–13283.

Geuze, H.J., Slot, J.W., Strous, G.J.A.M., Peppard, J., Von Figura, K., Hasilik, A., and Schwartz, A.L. (1984). Intracellular receptor sorting during endocytosis: comparative immunoelectron microscopy of multiple receptors in rat liver. Cell 37, 195–204.

Griffiths, G., and Gruenberg, J. (1991). The arguments for pre-existing early and late endosomes. Trends Cell Biol. 1, 5–9.

Gruenberg, J., Griffiths, G., and Howell, K.E. (1989). Characterization of the early endosome and putative carrier vesicles in vivo and with an assay of vesicle fusion in vitro. J. Cell. Biol. 108, 1301–1316.

Hansen, S.H., Olsson, A., and Casanova, J.E. (1995). Wortmannin, an inhibitor of phosphoinositide 3-kinase, inhibits transcytosis in polarized epithelial cells. J. Biol. Chem. 270, 28425–28432.

Hay, J.C., Fisette, P.L., Jenkins, G.H., Fukami, K., Takenawa, T., Anderson, R.A., and Martin, T.F.J. (1995). ATP-dependent inositide phosphorylation required for $Ca^{2+}$-activated secretion. Nature 374, 173–177.

Herman, P.K., and Emr, S.D. (1990). Characterization of VPS34, a gene required for vacuolar protein sorting and vacuole segregation in Saccharomyces cerevisiae. Mol. Cell. Biol. 10, 6742–6754.

Hiles, I.D., et al. (1992). Phosphatidylinositol 3-kinase: structure and expression of the 110 kD catalytic subunit. Cell 70, 419–429.

Joly, M., Kazlauskas, A., and Corvera, S. (1995). Phosphatidyl 3-kinase activity is required at a postendocytic step in platelet-derived growth factor receptor trafficking. J. Biol. Chem. 270, 13225–13230.

Joly, M., Kazlauskas, A., Fay, F.S., and Corvera, S. (1994). Disruption of PDGF receptor trafficking by mutation of its PI 3-kinase binding sites. Science 263, 684–687.

Jones, A.T., and Clague, M.J. (1995). Phosphatidylinositol 3-kinase activity is required for early endosome fusion. Biochem. J. 311, 31–34.

Klausner, R.D., Ashwell, G., Van Renswoude, J., Ashwell, G., Kempf, C., Schechter, A.N., Dean, A., and Bridges, K.R. (1983b). Receptor-mediated endocytosis of transferrin in K562 cells. J. Biol. Chem. 258, 4715–4724.

Klausner, R.D., Ashwell, G., Van Renswoude, J., Harford, J.B., and Bridges, K.R. (1983a). Binding of apotransferrin to K562 cells: explanation for the transferrin cycle. Proc. Natl. Acad. Sci. USA 80, 2263–2266.

Li, G., D'Souza-Schorey, C., Barbieri, M.A., Roberts, R.L., Williams, L.T., and Stahl, P.D. (1995). Evidence for phosphatidylinositol 3-kinase as a regulator of endocytosis via rab 5. Proc. Natl. Acad. Sci. USA 92, 10207–10211.

Mayorga, L.S., Colombo, M.I., Lennhartz, M., Brown, E.J., Rahman, K.H., Weiss, R., Lennon, P.J., and Stahl, P.D. (1993). Inhibition of endosome fusion by phospholipase $A_2$ (PLA2) inhibitors points to a role for PLA2 in endocytosis. Proc. Natl. Acad. Sci. USA 90, 10255–10259.

Munn, A.L., and Riezmann, H. (1994). Endocytosis is required for the growth of vacuolar $H^+$-ATPase-defective yeast: identification of six new END genes. J. Cell. Biol. 127, 373–386.

Murphy, R.F. (1991). Maturation models for endosome and lysosome biogenesis. Trends Cell. Biol. 1, 77–82.

Nakanishi, S., Catt, K.J., and Balla, T. (1995). A wortmannin-sensitive phosphatidyl 4-kinase that regulates hormone-sensitive pools of inositolphospholipids. Proc. Natl. Acad. Sci. USA 92, 5317–5321.

Ohashi, M., Jan de Vries, K., Frank, R., Snoek, G., Bankaitis, V., Wirtz, K., and Huttner, W.B. (1995). A role for phosphatidylinositol transfer protein in secretory vesicle formation. Nature 377, 544–547.

Okada, T., Kawano, Y., Sakakibara, T., Hazeki, O., and Ui, M. (1994). Essential role of phosphatidyl 3-kinase in insulin-induced glucose transport and antilipolysis in rat adipocytes. J. Biol. Chem. 269, 3568–3573.

Powis, G., et al. (1994). Wortmannin, a selective and potent inhibitor of phosphatidyl 3-kinase. Cancer Res 54, 2419–2423.

Robinson, M.S., and Kreis, T.E. (1992). Recruitment of coat proteins onto Golgi membranes in intact and permeabilized cells: effects of brefeldin A and G protein activators. Cell 69, 129–138.

Salzman, N.H., and Maxfield, F.R. (1988). Fusion accessibility of endocytic compartments along the recycling and lysosomal endocytic pathways in intact cells. J. Cell. Biol. 109, 2097–2104.

Scatchard, G. (1949). The attraction of proteins for small molecules and ions. Ann. NY Acad. Sci. 51, 660–672.

Schonhorn, J.E., and Wessling-Resnick, M. (1994). Brefeldin A down-regulates the transferrin receptor in K562 Cells. Mol. Cell. Biochem. 135, 159–169.

Schu, P.V., Takegawa, K., Fry, M.J., Stack, J.H., Waterfield, M.D., and Emr, S.D. (1993). Phosphatidylinositol 3-kinase encoded by yeast VPS34 gene essential for protein sorting. Science 260, 88–91.

Shepherd, P.R., Soos, M.A., and Siddle, K. (1995). Inhibitors of phosphoinositide 3-kinase block exocytosis but not endocytosis of transferrin receptors in 3T3-L1 adipocytes. Biochem. Biophys. Res. Commun. 211, 533–539.

Snider, M.D., and Rogers, O.C. (1985). Intracellular movement of cell surface receptors after endocytosis: resialylation of asialo-transferrin receptor in human erythroleukemia cells. J. Cell. Biol. 100, 826–834.

Stack, J.H., DeWald, D.B., Takegawa, K., and Emr, S.D. (1995). Vesicle-mediated protein transport: regulatory interactions between

the Vps15 protein kinase and the Vps34 PtdIns 3-kinase essential for protein sorting to the vacuole in yeast. J. Cell Biol. *129*, 321–334.

Stack, J.H., and Emr, S.D. (1994). VPS34p required for yeast vacuolar protein sorting is a multiple specificity kinase that exhibits both protein kinase and phosphatidylinositol-specific PI 3-kinase activities. J. Biol. Chem. *269*, 31552–31562.

Stack, J.H., Herman, P.K., Schu, P.V., and Emr, S.D. (1993). A membrane-associated complex containing the Vps15 protein kinase and the Vps34 PI 3-kinase is essential for protein sorting to the yeast lysosome-like vacuole. EMBO J. *12*, 2195–2204.

Stein, B.S., and Sussman, H.H. (1986). Demonstration of two distinct transferrin receptor recycling pathways and transferrin-independent receptor internalization in K562 cells. J. Biol. Chem. *261*, 10319–10331.

Stephens, L., Smrcka, A., Cooke, F.T., Jackson, T.R., Sternweis, P.C., and Hawkins, P.T. (1994). A novel phosphoinositide 3-kinase activity in myeloid-derived cells is activated by G proteins $\beta\gamma$ subunits. Cell *77*, 83–93.

Stoyanov, B., *et al.* (1995). Cloning and characterization of a G protein-activated human phosphoinositide 3-kinase. Science *269*, 690–693.

Volinia, S., Dhand, R., Vanhaesebroeck, B., MacDougall, L.K., Stein, R., Zvelebil, M.J., Domin, J., Panaretou, C., and Waterfield, M.D. (1995). A human phosphatidylinositol 3-kinase complex related to the yeast Vps34p-Vps15p protein sorting system. EMBO J. *14*, 3339–3348.

Wessling-Resnick, M., and Braell, W.A. (1990). The sorting and segregation mechanism of the endocytic pathway is functional in a cell-free system. J. Biol. Chem. *265*, 690–699.

Wiley, H.S, and Cunningham, D.D. (1982). The endocytic rate constant. J. Biol. Chem. *257*, 4222–4229.

Yamamoto, A., DeWald, D.B., Borenkov, I.V., Anderson, R.A., Emr, S.D., and Koshland, D. (1995). Novel PI(4)P 5-kinase homologue, Fab1p, essential for normal vacuole function and morphology in yeast. Mol. Biol. Cell *6*, 525–539.

Yamashiro, D.J., and Maxfield, F.R. (1987). Acidification of morphologically distinct endosomes in mutant and wild-type Chinese hamster ovary cells. J. Cell. Biol. *105*, 2723–2733.

Yamashiro, D.J., Tycko, B., Fluss, S.R., and Maxfield, F.R. (1984). Segregation of transferrin to a mildly acidic (pH 6.5) para-Golgi compartment in the recycling pathway. Cell *37*, 789–800.